agronomy

MDPI

Article

Soil Microbes from Saline–Alkali Farmland Can Form Carbonate Precipitates

Zhen Liu [1,2,*], Jing Li [1,2], Yitao Zhang [1,2], Huarui Gong [1,2], Ruixing Hou [1], Zhigang Sun [1,2,3] and Zhu Ouyang [1,2,3]

[1] CAS Engineering Laboratory for Yellow River Delta Modern Agriculture, Institute of Geographic Sciences and Natural Resources Research, Chinese Academy of Sciences, Beijing 100101, China
[2] Shandong Dongying Institute of Geographic Sciences, Dongying 257000, China
[3] University of Chinese Academy of Sciences, Beijing 100049, China
* Correspondence: liuzhen@igsnrr.ac.cn; Tel.: +86-132-6983-8513

Abstract: The formation of soil inorganic carbon in saline–alkali lands is of great significance for enhancing soil carbon sequestration. As for the formation mechanisms, in addition to the discovered abiotic mechanisms, the microbial mechanisms remain unclear. To address this, soil microbes were isolated from the saline–alkali farmland of the Yellow River Delta in north China. Then, their capacity for carbonate precipitation formation was determined. Ten microbial strains were obtained from the soil. Of these, seven strains (four bacterial strains and three fungal strains), belonging to *Rhodococcus* sp., *Pseudomonas* sp., *Bacillus* sp., *Streptomyces* sp., *Aspergillus* sp., *Cladosporium* sp., and *Trichoderma* sp., formed carbonate precipitates in the range of 89.77~383.37 mg. Moreover, the formation of carbonate precipitates was related to specific metabolisms by which microbes can raise the pH (from 7.20 to >8.00), suggesting that soil microbes that can enhance pH values by specific metabolisms containing the function of carbonate formation. Although an in situ experiment is needed to confirm such capacity, these results showed that soil bacteria and fungi existing in the saline–alkali farmland soil can form carbonate precipitates. The present study provided a microbial perspective for the mechanism of soil inorganic carbon formation, further implying a microbial potential of soil carbon sequestration in saline–alkali farmlands.

Keywords: saline–alkali soil; soil inorganic carbon; carbonate formation; soil bacteria; soil fungi

Citation: Liu, Z.; Li, J.; Zhang, Y.; Gong, H.; Hou, R.; Sun, Z.; Ouyang, Z. Soil Microbes from Saline–Alkali Farmland Can Form Carbonate Precipitates. *Agronomy* **2023**, *13*, 372. https://doi.org/10.3390/agronomy13020372

Received: 23 December 2022
Revised: 20 January 2023
Accepted: 22 January 2023
Published: 27 January 2023

1. Introduction

The global saline–alkali land area occupies approximately 1.13×10^9 hm^2, including salinized desert, salinized land, and coastal saline–alkali land [1]. In recent years, it has been found that saline–alkali lands store large amounts of soil inorganic carbon, including primary and secondary carbonates [2]. Since its storage is larger than that of soil organic carbon [3], and the time that carbon resides in soil inorganic carbon is much longer than that in soil organic carbon [4], the accumulation of soil inorganic carbon in saline–alkali lands thus plays an important role in the ecosystem's carbon cycle. Against the background of intensified human activities and global climate changes, a thorough understanding of the formation and accumulation process of soil inorganic carbon is of great significance for a comprehensive understanding of soil carbon sink potential in saline–alkali lands.

The phenomena of formation and accumulation of carbonate precipitates in saline–alkali farmlands have been found with crop planting and vegetation restoration [5]. Several abiotic mechanisms are considered to play an important role in such carbon transformation and have been widely investigated. Specifically, CO_2 originating from root respiration and litter decomposition can be transformed into soil carbonate precipitates through the processes of CO_2 dissolution and precipitation (Equations (1) and (2)) [6,7]. Since CO_2 dissolves in soil water to form H^+ (which is acidic), the continuous process of CO_2 dissolution may inhibit the formation of carbonate precipitates; thus, this process may not

continue in saline–alkali soil. Moreover, some studies have reported that the dissolution process of soil carbonate precipitates can sequestrate CO_2 (Equation (3)), which increases soil inorganic carbon storage [8]. As the soluble inorganic carbon (mainly HCO_3^-) content in saline–alkali soil is much lower than the total inorganic carbon content [4], even if the process stores CO_2, it cannot form a large number of carbonate precipitates. When soil water content decreases, the stored CO_2 may be re-released from the soil to some extent. Furthermore, weathering processes of silicate, aluminosilicate, and other minerals in soil are also considered a pathway for fixing CO_2 and forming carbon-containing minerals [4]. Considering the low rate of the weathering [9,10], its contribution to the accumulation of soil inorganic carbon during the periods of plant growth should be very small [11].

$$CO_2+H_2O \leftrightarrow H^+ + HCO_3^- \leftrightarrow CO_3^{2-} + 2H^+ \quad (1)$$

$$Ca^{2+} + CO_3^{2-} \leftrightarrow CaCO_3 \quad (2)$$

$$CaCO_3 + CO_2 + H_2O \leftrightarrow Ca^{2+} + 2HCO_3^- \quad (3)$$

$$NH_3 + H_2O \leftrightarrow NH_4^+ + OH^- \quad (4)$$

$$13H^+ + 8NO_3^- + 5CH_3COO^- \rightarrow 4N_2 + 10CO_2 + 14H_2O \quad (5)$$

$$CO_3^{2-} + Ca^{2+} \xrightarrow{\text{microbe}} CaCO_3 \quad (6)$$

Since saline–alkali soil is considered a complex heterogeneous system, the formation of soil inorganic carbon may contain both abiotic and microbial mechanisms due to the processes of interaction and coupling in the soil [12]. Many studies have confirmed that soil microbes play an important role in the formation of soil inorganic carbon [12–14]. To date, it has been difficult to clarify the role of soil microbes in saline–alkali soil. Recently, soil microbes containing the capacity of forming carbonate precipitates have been discovered in various conditions, e.g., desert soils, water, and caves [12–14]. These microbes increase the pH value and the content of CO_3^{2-} in the microdomain through metabolic processes such as urea hydrolysis, ammonization (Equation (4)), denitrification (Equation (5)), and sulfate reduction processes, thereby forming carbonate precipitates, e.g., calcium carbonate ($CaCO_3$) (Equation (6)). Some studies have shown that, even in harsh saline–alkali lands, soil microbes play an important role in the process of material conversion [15–17]. As for the mechanisms for the formation of soil inorganic carbon, in addition to the discovered abiotic mechanisms [2,3,8], microbial mechanisms should not be ignored. However, few studies have been conducted on the presence of soil microbes capable of carbonate precipitates formation in saline–alkali soils. This represents an important gap in our knowledge of the formation of soil inorganic carbon in saline–alkali lands via microbial mechanisms.

Therefore, it is necessary to explore the capacity of soil microbes from saline–alkali farmland soil to form carbonate precipitates. We hypothesized that soil microbes in saline–alkali soil contain the capacity of forming carbonate precipitates. To address this, soil microbes were isolated from the saline–alkali soil of the Yellow River Delta (YRD) in northern China. Then, their capacity for carbonate precipitation was determined under controlled conditions. The present study provides an important case supporting the microbial mechanisms involved in soil inorganic carbon formation in saline–alkali lands.

2. Materials and Methods

2.1. Site Description and Sampling Collection

The study was conducted at the lower YRD of the Shandong Province, China (37°40′ N, 118°55′ E; 1 m above sea level). The region has a temperate continental monsoon climate, with 530–630 mm mean annual precipitation, 1962 mm annual evaporation, and 12.40 °C mean temperature [18,19]. The region is located in the south of North China and Bohai Basin, which is a Cenozoic sedimentary basin. The sedimentary thickness of coastal lacustrine facies and fluvial facies is up to 7000 m. The soil in this region has been deposited by the Yellow River sediment since 1855, so no stratification is found in the surface soil.

Accordingly, the region has a generally young soil in alluvial deposits, and the main soil type is Calcaric Fluvisols [20]. The mineral composition of the soil is carbonate minerals (calcite and dolomite, 13.99%), quartz (42.44%), feldspar (potassium feldspar and plagioclase, 27.88%), clay minerals (illite and chlorite, 14.22%), and hornblende (1.25%). The original vegetation is dominated by the halophytic species, such as *Artemisia scoparia*, *Phragmites communis*, *Tamarix chinensis*, and *Suaeda glauca*, along a disparate salinity gradient. In recent years, the research site has undergone intensive conversion from natural land to agricultural field (Figure 1). The crops, including *Sorghum bicolor* (L.) *Moench* and *Zea mays* Linn, are mainly promoted with the comprehensive utilization of the coastal saline–alkali lands. Soil water content is about 10.60 m^3 m^{-3}. The soil (with a depth of 0–20 cm) in the research site contains 0.12% clay, 19.99% silt, and 79.89% sand [21]. Soil organic matter content is about 5.00 g kg^{-1}. Soil inorganic carbon content is about 8.31 g kg^{-1}. Soil total nitrogen content is about 0.54 g kg^{-1}. Soil alkali-hydrolysable nitrogen is about 38.75 mg kg^{-1}. Soil pH is about 8.48. Electrical conductivity (EC) is about 2.66 ms cm^{-1}. The main soil ions, including the bicarbonate, sulfate, chlorine ion, calcium ion, magnesium ion, potassium ion, and sodium ion, are about 502.18 mg kg^{-1}, 1522.40 mg kg^{-1}, 3211.27 mg kg^{-1}, 1040.00 mg kg^{-1}, 553.07 mg kg^{-1}, 249.36 mg kg^{-1}, and 8.92 mg kg^{-1}, respectively.

Figure 1. Photographs of the research site and sampling plots.

In July 2021, six 20 m × 20 m sampling plots were selected from the dry saline–alkali farmland within 1 km × 1 km in the research site (Figure 1). In each sampling plot, six soil cores were randomly obtained from a depth range of 0–20 cm using a sterilized soil auger and mixed as a representative sample. The sample was screened through a 2 mm soil sieve to remove plant litter and roots and divided into two parts for subsequent analysis. One part was stored at 4 °C conditions for isolating microbial strains. A second was used for obtaining soil extract with a ratio of soil–water of 1:1.

2.2. Isolation and Identification of Saline–Alkali Soil Microbes

For each sample, 1.0 g of fresh soil was mixed with 10 mL of sterilized deionized water by shaking it for 10 min to form a uniform suspension. Then, using the gradient dilution method, the soil suspension was diluted 10^{-3} times for the following isolation of microbial strains steps [17]. A total of 100 µL of the diluted suspension, as the inoculum, was spread on the sterilized mineral salt medium (MSM) at pH 7.25, and the same amount of autoclaved suspension was used as the control. MSM contained $Na_2HPO_4{\cdot}2H_2O$, 3.5 g L^{-1}; KH_2PO_4, 1.0 g L^{-1}; $(NH_4)_2SO_4$, 0.5 g L^{-1}; $MgCl_2{\cdot}6H_2O$, 0.1 g L^{-1}; $Ca(NO_3)_2{\cdot}4H_2O$, 0.05 g L^{-1}; trace elements, 1 mL L^{-1}; and 1 L of soil extract with a ratio of soil–water of 1:1 on 1.5% agar. This MSM was used to simulate the oligotrophic and high salt conditions of the saline–alkali soil [17]. All plates were incubated at 25 °C for two weeks. Microbial colonies growing on the plates were differentiated morphologically and were picked and coated onto Luria–Bertani plates for further isolation and purification to obtain bacterial and

fungi strains. This process was repeated several times until pure microbial isolations were obtained. The obtained isolations were identified and used for the following experiments.

A genomic DNA sample (1 µL) from each isolation was obtained using the Genome DNA kit (Qiagen Inc., Germantown, MD, USA), following the manufacturer's instructions. The DNA samples of the bacterial and fungi strains were amplified using PCR analyses with the primer pairs of 27F/1492R and ITS1/ITS4, respectively. The reaction conditions for amplification were carried out as follows: 5 min initial denaturation at 95 °C, followed by 30 cycles of 20 s denaturation at 95 °C, 30 s primer annealing at 50 °C, and 3 min extension at 60 °C. The amplified DNA was purified using Qiaquick PCR Purification Kit (Qiagen Inc., Germantown, MD, USA) and sequenced. The 16S rDNA gene sequence of the bacterial strain and ITS gene sequence of the fungal strain were identified by BLAST analysis using the National Center for Biotechnology Information (NCBI) database. The strain in the present study represents the obtained purebred population and its progeny that are derived from an isolated single cell, which is a sign that a microbe has attained genotypic purity. The phylogenetic tree was constructed based on the neighbor-joining method and 2000 boot-up replication by combining with MEGA7.0 software [22]. The maximum composite likelihood method was further used to calculate the evolutionary distance and finally determine the membership of the obtained strain. Nucleotide sequences were submitted to GenBank with the accession numbers OQ101595-OQ101601 and OQ101609-OQ101611.

2.3. Processes of Microbial Carbonate Formation and Identification

To determine the ability of carbonate formation of the obtained bacteria and fungi, a controlled cultural experiment was conducted. Specifically, each strain was inoculated in 100 mL of liquid cultural medium in a 250 mL triangular flask in triplicate at 25 °C. The groups inoculated with autoclaved isolations were conducted as the control group. The medium contained tryptone 10 g L^{-1}, yeast extract 5 g L^{-1}, sodium chloride 10 g L^{-1}, and calcium chloride 5 g L^{-1}, with a pH of 7.20. The bottom of the flasks was observed every week to determine the number of precipitates formed after nine weeks. After the incubation, the liquid culture medium was collected and used to analyze the pH, EC, dissolved ammonium nitrogen (NH_4^+-N), and nitrate nitrogen (NO_3^--N). The precipitates in the flask were collected, oxidated with 10% hydrogen peroxide to remove adhesive impurities, washed with sterilized distilled water, air-dried at room temperature [12,17], and weighed using an electronic balance (ME104E, Mettler Toledo, Greifensee, Switzerland). The pH was determined using a pH meter (FE28, Mettler Toledo, Greifensee, Switzerland). EC was determined using a conductivity meter (FE38, Mettler Toledo, Greifensee, Switzerland). NH_4^+-N content (c(NH_4^+-N)) and NO_3^--N content (c(NO_3^--N)) were determined by ultraviolet spectrophotometry (UV-2700, SHIMADZU, Kyoto, Japan). To identify the crystals of the precipitate, a scanning electron microscope (SEM; Quanta 650, FEI, Portland, OR, USA) was used to analyze the morphology of the precipitate, and an energy spectrum analyzer (EDS; Quanta, Bruker, Bremen, Germany) was used to analyze the element composition information. The crystal type and composition of the precipitate were analyzed by an X-ray diffraction analyzer (XRD; D8 Advance, Bruker Biospin, Ettlingen, Germany).

2.4. Data Analysis and Processing

A one-way analysis of variance (ANOVA) and Tukey's HSD post hoc test were conducted to analyze the difference in the weight of the precipitates produced by the strains, pH, EC, c(NH_4^+-N), and c(NO_3^--N) among the different media using the base package of R statistical software [23]. In addition, Student's *t*-test was employed to determine the difference in these data between the incubated and control groups. Moreover, Pearson correlation analysis was conducted to determine the relationships among the weight of precipitates, pH, EC, c(NH_4^+-N), and c(NO_3^--N). All statistical analyses were performed using R version 4.0.3 [23]. Statistical significance was indicated by $p < 0.05$.

3. Results

3.1. Isolation and Identification of the Microbial Strains

After DNA sequencing and identification, 10 microbial strains (Figure 2) were obtained from the cultural media, of which 7 were bacteria and designated as strains 1–7 and 3 strains were fungi, designated as strains 8–10. On the basis of the phylogenetic analysis and NCBI results, strain 1 belonged to *Rhodococcus* sp. (>99% homology with *Rhodococcus* sp. strain S2–17); strain 2 to *Pseudomonas* sp. (>99% homology with *Pseudomonas* sp. G22); strain 3 to *Pseudomonas* sp. (>99% homology with *Pseudomonas corugata* strain 155-HR9); strain 4 to *Pseudomonas* sp. (>99% homology with *Pseudomonas* sp. F4 (2014)); strain 5 to *Phyllobacterium* sp. (>99% homology with *Phyllobacterium ifriqiyense* strain TRM85142); strain 6 to *Bacillus* sp. (>99% homology with *Bacillus* sp. strain XA15-41); and strain 7 to *Streptomyces* sp. (>99% homology with *Streptomyces* sp. XAS585). In addition, strain 8 belonged to *Aspergillus* sp. (>99% homology with *Aspergillus sydowii* isolate EO_4); strain 9 to *Cladosporium* sp. (>99% homology with *Cladosporium tenuissimum* strain CIFRI); and strain 10 to *Trichoderma* sp. (>99% homology with *Trichoderma* sp. isolate SDAS203637).

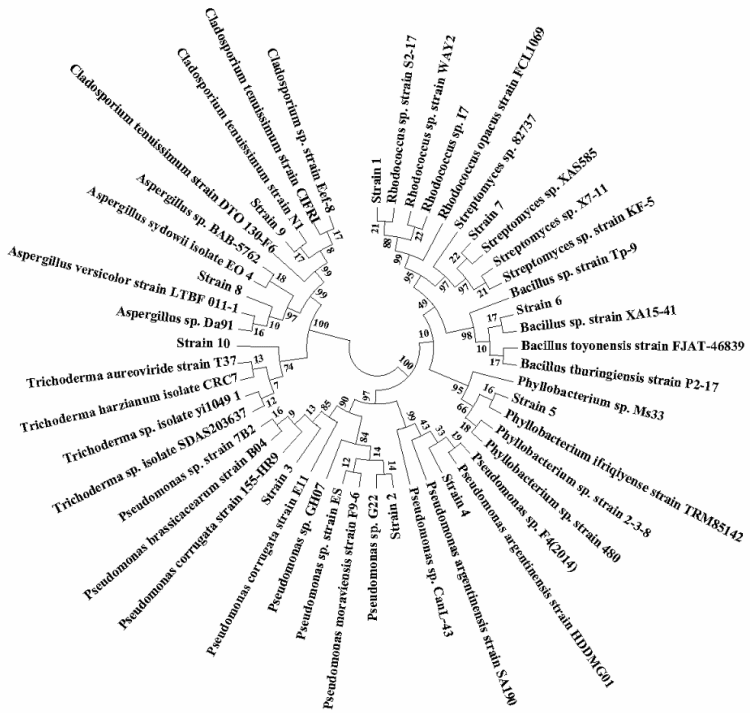

Figure 2. Phylogenetic diagram of the isolated strains.

3.2. Precipitate Formation and Physicochemical Properties' Variation in the Cultural Media

After the cultural experiment was conducted, the precipitates formed were collected (Figure 3). Culture media with strains 1, 2, 6, 7, 8, 9, and 10 formed precipitates, while strains 3, 4, and 5 did not. The precipitates produced by strains 1–2 and 6–10 were 280.80, 380.37, 325.97, 207.53, 326.97, 203.60, and 89.77 mg, respectively. No precipitate was found in the control groups. Additionally, a significant difference was found among the weight of precipitates formed by the strains ($p < 0.01$).

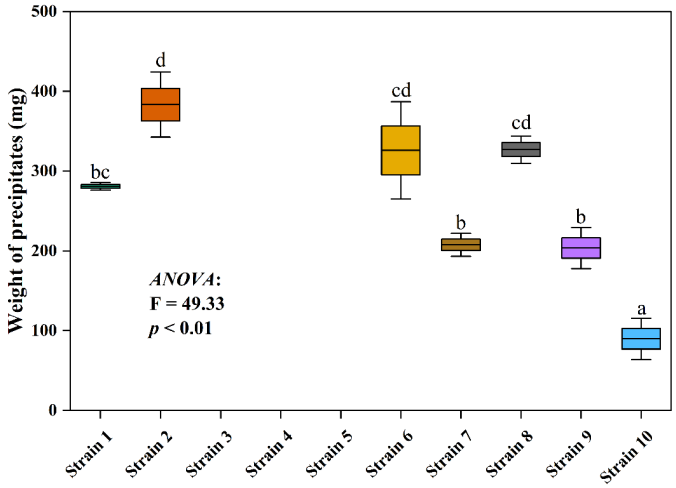

Figure 3. Weight of the precipitates in the culture media formed by the different strains. The line in the middle of the box and the error bar represents the mean value and the standard deviation of the weight of the precipitates, respectively. Different letters indicate a significant difference in the weight of the precipitates in the culture media formed by the different strains (Tukey's HSD; $p < 0.05$). Different colors in the box indicate the different culture media. ANOVA, Analysis of Variance.

In the culture media forming precipitates, the pH and c(NH_4^+-N) of the cultural group were significantly higher than that of the control group, while the variations in the EC and c(NO_3^--N) were significantly opposite (Figure 4, $p < 0.05$). In the culture media without precipitate, no significant difference was found in the pH and EC between the two groups ($p > 0.05$); however, c(NH_4^+-N) and c(NO_3^--N) of the cultural group were significantly higher and lower, respectively, than that of the control group ($p < 0.05$). Moreover, the ANOVA analysis showed that strain types had significant effects on the pH, EC, c(NH_4^+-N), and c(NO_3^--N) among the culture media ($p < 0.05$), and for the EC and c(NO_3^--N) in the control groups ($p < 0.05$). However, no effect of strain types on the pH and c(NH_4^+-N) was determined in the control groups ($p > 0.05$).

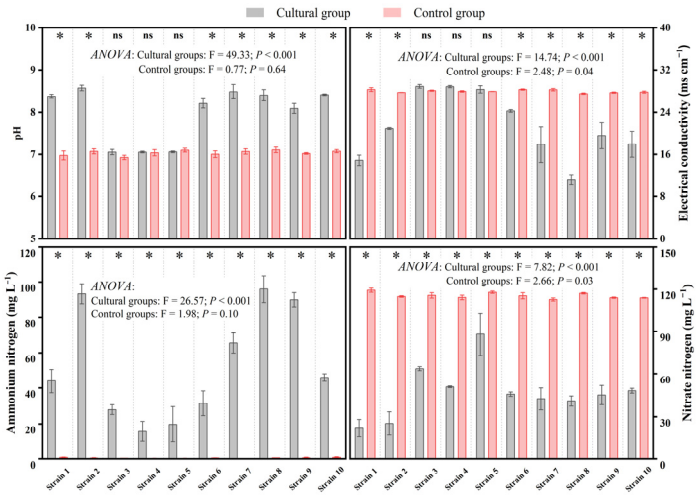

Figure 4. Physicochemical properties of the culture media. The asterisk indicates significant difference between the culture and control groups; ns indicates not. ANOVA, Analysis of Variance.

Correlation analysis showed that, in all media (Table 1), the weight of precipitates was significantly positively correlated with the pH and c(NH_4^+-N) and remarkably negatively correlated with the EC and c(NO_3^--N). In addition, pH, EC, c(NH_4^+-N), and c(NO_3^--N) among the culture media were significantly correlated with each other ($p < 0.05$).

Table 1. Correlation among the weight of the precipitates and physicochemical properties.

	Weight of Precipitates	pH	EC	$c(NH_4^+)$
pH	0.82 ***			
EC	−0.63 ***	−0.81 ***		
$c(NH_4^+)$	0.69 ***	0.70 ***	−0.66 ***	
$c(NO_3^-)$	−0.68 ***	−0.72 ***	0.59 ***	0.55 **

$c(NH_4^+)$, ammonium nitrogen content; $c(NO_3^-)$, nitrate nitrogen content. EC, Electrical conductivity. ** and *** indicate a significant correlation at the levels of 0.01 and 0.001, respectively.

3.3. Identification of the Precipitates Formed by the Microbes

The SEM results of the precipitates are shown in Figure 5. The surface structures of the precipitates produced by strains 1, 2, 6, 7, 8, 9, and 10 were diverse. Most of the precipitates were in hemispherical and lamellar structures with multiple layers and rough surfaces, also known as botryoidal structures. The structures of holes and sheath were observed on the surface of the precipitates, which is the trace left by the survival of microbes. Additionally, different strains formed various precipitates in terms of the shapes and structures. For example, the precipitates formed by strain 1 were bound together in a hemispherical manner with fewer pores on its surface. The precipitates formed by strain 6 were spherical, with a rough surface. Holes and wrapping sheaths left by microbes were observed. However, the precipitates formed by strain 10 were present the rough surface, mostly composed of layers and sheets, with many holes.

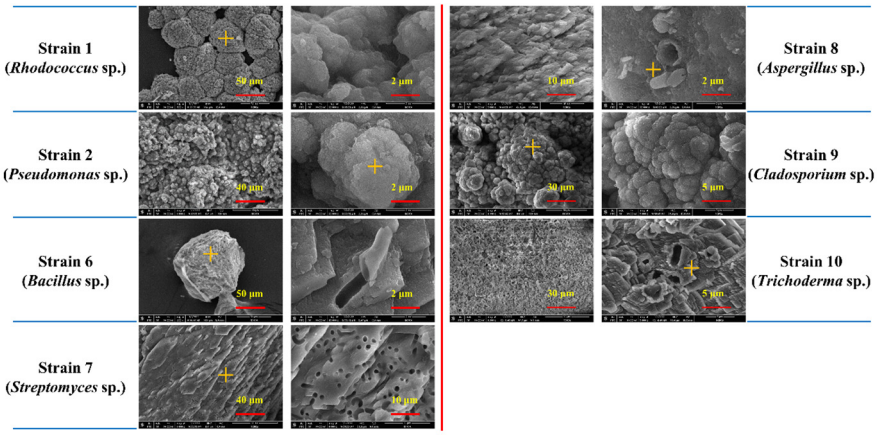

Figure 5. Scanning electron microscopy of the minerals formed by the strains. The yellow cross represents the location of the EDS analysis performed.

Additionally, the elemental composition of the precipitate was analyzed by EDS (Table 2). The atomic and mass percentages of carbon, oxygen, and calcium were 19.53~26.80%, 58.90~61.61%, 11.84~17.21% and 12.12~17.92%, 51.07~55.41%, 26.67~35.62%, respectively, close to the atomic and mass percentages of the corresponding elements in $CaCO_3$, namely, 1:3:1 and 12:48:40, respectively. Therefore, the precipitates were preliminarily determined as the crystal of $CaCO_3$. Furthermore, the XRD analysis of the crystal type shows that it was a variety of $CaCO_3$ isomers, mainly calcite and vaterite (Table 2). Calcite is a stable polymorph of $CaCO_3$, while vaterite is an unstable polymorph. Among them, most of the $CaCO_3$ formed by strains 1 and 7 were vaterite, followed by calcite; approximate 50% calcite and vaterite accounted for approximate 50% each formed by strains 2, 8, and 9; strains 6 and 10 were only found to form calcite.

Table 2. Mineral element composition and crystal composition of precipitates.

Strain Types	Element Composition						Crystal Types	
	Atom Percentage (%)			Quality Percentage (%)			Calcite	Vaterite
	Carbon	Oxygen	Calcium	Carbon	Oxygen	Calcium	%	%
1	25.52	59.64	14.83	16.52	51.43	32.05	18.90	81.10
2	26.54	61.61	11.84	17.92	55.41	26.67	46.70	53.30
6	25.87	60.84	13.29	17.11	53.58	29.31	100	-
7	23.17	60.60	16.24	14.66	51.07	34.28	10.70	89.30
8	19.53	63.26	17.21	12.12	52.27	35.62	55.90	44.10
9	26.80	58.90	14.30	17.52	51.29	31.19	42.70	57.30
10	23.88	61.17	14.96	15.38	52.47	32.15	100	-

4. Discussion

The precipitates were found in the culture group cultivating strains (Figure 2), while no such substance was found in the control groups. Additionally, the specific surface structures of the precipitates, including the pores, wrapping sheaths, multiple layers, and rough surfaces (Figure 5), in the present study were confirmed that those signs usually appear on the carbonate precipitates formed by microbes [17,24–26]. As hypothesized, these results together suggest that some soil bacteria and fungi from the saline–alkali farmland contained the capacity to induce the formation of carbonate precipitates. Moreover, the results show that, among the 10 strains isolated from saline–alkali farmland soils, 7 strains, that is, 4 bacterial strains and 3 fungal strains, contained the ability to form carbonate precipitates (Figures 2 and 3), belonging to the genera *Rhodococcus*, *Pseudomonas*, *Bacillus*, *Streptomyces*, *Aspergillus*, *Cladosporium*, and *Trichoderma*. However, only one of the three isolated *Pseudomonas* strains produced carbonate precipitates (Figure 3), which indicates that, although strains in the same genus have similar genetic characteristics, their specific functions may be different. The predicted specific functions through genetic characteristics still need empirical experiments to verify them. In view of this, although microbial strains belonging to the genera *Rhodococcus*, *Pseudomonas*, *Bacillus*, and *Streptomyces* contained the capacity of forming carbonate precipitates and have been found in deserts, caves, water, and other environments [17,27–31], our results provide the microbial empirical case that these genera have large numbers of microbes capable of carbonate precipitate formation. These results further extend the understanding of the role of microbes in carbon cycling in the saline–alkali farmland to some extent.

The results demonstrate that increment trends in the pH and c(NH_4^+-N) and decrement trends in the EC and c(NO_3^--N) in the culture media forming precipitates compare with the culture media without precipitates (Figure 4). Therefore, it can be speculated that the increment in pH may be caused by the specific microbial metabolisms, for example, amino acid deamination and/or denitrification processes (Equations (4) and (5)). The increased pH would provide sufficient carbonate and bicarbonate for the formation of carbonate precipitates [32]. On the basis of the above results, the microbial carbonate formation process can be inferred that the microbes absorb calcium ions, increasing the concentration of calcium ion in their living conditions. In addition, the specific metabolic processes increase the pH of the culture media, which provides sufficient carbonate for the carbonate formation, so that the ion concentration in microbial microdomain exceeds the solubility of $CaCO_3$ and then forms carbonate precipitates (Equation (6)). This also indicates that the formation of soil inorganic carbon in saline–alkali soils may be a combination of microbial and abiotic processes, that is, soil microbes transform CO_2 from plants and atmosphere into soil carbonate and bicarbonate through specific metabolic processes, which promotes the formation of supersaturated ion concentration of carbonate precipitates in the situation where soil microbes live, hence forming soil carbonate precipitates [12,33]. On the basis of this, these results further provide a microbial clue for the formation mechanism of inorganic carbon in saline–alkali farmland soil.

Many studies have investigated the bacterial ability forming carbonate precipitates [12,24–33]. As far as we know, the results firstly exhibit that fungal strains, belonging to *Aspergillus*, *Cladosporium*, and *Trichoderma*, isolated from saline–alkali farmland soil, contain the capacity of forming carbonate minerals (Figure 2), which extends the understanding of the carbon metabolism process of fungi in saline–alkali soils [34–36]. The capacity of carbonate precipitate formation may be a passive protection mechanism for fungi to adapt to the saline–alkali surroundings [34,37]. Because the high content of calcium ions in saline alkali soil (1040 mg kg^{-1} in the research site) will lead to toxic effects on fungal cells, the calcium ion content could be reduced in the micro-surroundings by forming the carbonate precipitates [34,37]. In view of this, a significant number of soil fungi that can form carbonate minerals may exist in saline–alkali soils. It has also been found that crops growing in saline–alkali soil can produce a large amount of calcium oxalate in their bodies to resist stress [38]. Such substances could be metabolized and utilized by some fungi to generate carbonate precipitates [34–37], which proves that soil fungi in saline–alkali soil may play a very important role in the formation of carbonate precipitates. In the present study, 10 strains were isolated on the basis of specific culture media, 7 of which contain the capacity of forming carbonate precipitates. In the future, more microbes with such function may be obtained through other culture media.

Strains 1–2 and 6–10 can convert 62.34%, 85.11%, 72.36%, 46.07%, 72.59%, 45.20%, and 19.93% of soluble calcium ions into calcium in $CaCO_3$ under the culture conditions on the basis of the calculation of calcium ion mass conservation (Figure 3). Therefore, it can be inferred that these strains contain high efficiency for forming carbonate precipitates in saline–alkali conditions through the specific metabolisms. Although the nutrient content of saline–alkali farmland soil is low, sufficient nitrogen-rich substances could also be input into the soil through the input of plant roots and the application of organic fertilizer [5,6]. The present study utilized such substances to simulate the process related to nitrogen metabolism that may occur in saline–alkali farmland soils by microbes. These metabolic processes have been confirmed by relevant studies to occur in the soil [12,39], transforming the CO_2 from soil organic matter and atmosphere into carbonate precipitates. Additionally, saline–alkali farmland soil can provide sufficient cations for microbes to form carbonate precipitates [5], including calcium ions and magnesium ions (1040.00 and 553.07 mg kg^{-1} in the present study, respectively) due to the high background values, input of fertilization, surface water irrigation, and other processes. Therefore, sufficient substances for soil microbes to form carbonate precipitates exist in the saline–alkali farmland soil. Although the results verify the ability of bacterial and fungal strains forming carbonate precipitates under cultivation conditions, whether carbonate precipitates can be formed by these strains in saline–alkali farmland soil and at what rate still need to be verified in situ. Nevertheless, our results firstly confirm that bacteria and fungi can form carbonate precipitates in the saline–alkali farmland soil. On the basis of the speculated metabolic process, the formation of secondary inorganic carbon in saline–alkali soil may be the result of the joint action of biotic and abiotic processes. The present study provides a microbial perspective for the mechanism of inorganic carbon formation in the saline–alkali farmland soil, further implying a potential of microbial pathway of soil carbon sequestration in saline–alkali lands.

5. Conclusions

To determine the capacity of microbes in saline–alkali farmland soil for carbonate precipitates formation, soil microbes were isolated from the saline–alkali farmland soil in the YRD in northern China, and a further test was conducted to see whether the microbes contain the function of forming carbonate precipitates. The results show that, among the 10 strains isolated, 7 strains, including 4 bacteria and 3 fungi strains, formed carbonate precipitates. The weight of carbonate precipitates was related to the metabolic processes that can improve the pH value in their living conditions, suggesting that microbial species that can enhance the pH values by specific metabolisms contain the function of carbonate precipitate formation. Nevertheless, our results exhibit that not only the soil bacteria but

also the fungi contain the function of carbonate precipitate formation, thus expanding the understanding that such formation processes are mostly related to bacterial metabolisms. Although the potential of these microbes to form carbonate in these soil conditions still needs to be explored, this study provides a microbial perspective for the mechanism of soil inorganic carbon formation in saline–alkali farmland soil.

Author Contributions: Conceptualization, methodology, investigation, resources, data curation, project administration, formal analysis, writing—original draft preparation, Z.L., J.L., Y.Z. and H.G.; funding acquisition, writing—review and editing, Z.L., R.H., Z.S. and Z.O. All authors have read and agreed to the published version of the manuscript.

Funding: This work was supported by the National Natural Science Foundation of China (no. 32101392), the Shandong Provincial Natural Science Foundation (no. ZR2021QC055), and the Strategic Priority Research Program of Chinese Academy of Sciences (no. XDA26050202).

Data Availability Statement: The data presented in this study are available on request from the corresponding author. The data are not publicly available due to privacy restrictions.

Acknowledgments: Thanks to Mengyun Cai for her encouragement and help in my work.

Conflicts of Interest: The authors declare no conflict of interest.

References

1. Wicke, B.; Smeets, E.; Dornburg, V.; Vashev, B.; Gaiser, T.; Turkenburg, W.; Faaij, A. The global technical and economic potential of bioenergy from salt-affected soils. *Energy Environ. Sci.* **2011**, *4*, 2669–2681. [CrossRef]
2. Wang, X.; Wang, J.; Xu, M.; Zhang, W.; Fan, T.; Zhang, J. Carbon accumulation in arid croplands of northwest China: Pedogenic carbonate exceeding organic carbon. *Sci. Rep.* **2015**, *5*, 11439. [CrossRef] [PubMed]
3. Guo, Y.; Wang, X.; Li, X.; Wang, J.; Xu, M.; Li, D. Dynamics of soil organic and inorganic carbon in the cropland of upper Yellow River Delta, China. *Sci. Rep.* **2016**, *6*, 36105. [CrossRef] [PubMed]
4. Monger, H.C.; Kraimer, R.A.; Khresat, S.E.; Cole, D.R.; Wang, X.; Wang, J. Sequestration of inorganic carbon in soil and groundwater. *Geology* **2015**, *43*, 375–378. [CrossRef]
5. Zhu, Y.; Wang, Y.; Guo, C.; Xue, D.; Li, J.; Chen, Q.; Song, Z.; Lou, L.; Kuzyakov, Y.; Wang, Z.L.; et al. Conversion of coastal marshes to croplands decreases organic carbon but increases inorganic carbon in saline soils. *Land Degrad. Dev.* **2020**, *31*, 1099–1109. [CrossRef]
6. Kim, J.H.; Jobbágy, E.G.; Richter, D.D.; Trumbore, S.E.; Jackson, R.B. Agricultural acceleration of soil carbonate weathering. *Glob. Change Biol.* **2020**, *26*, 5988–6002. [CrossRef]
7. Hasinger, O.; Spangenberg, J.E.; Millière, L.; Bindschedler, S.; Cailleau, G.; Verrecchia, E.P. Carbon dioxide in scree slope deposits: A pathway from atmosphere to pedogenic carbonate. *Geoderma* **2015**, *247*, 129–139. [CrossRef]
8. Wang, X.; Jiang, Z.; Li, Y.; Kong, F.; Xi, M. Inorganic carbon sequestration and its mechanism of coastal saline-alkali wetlands in Jiaozhou Bay, China. *Geoderma* **2019**, *351*, 221–234. [CrossRef]
9. Sanderman, J. Can management induced changes in the carbonate system drive soil carbon sequestration? A review with particular focus on Australia. *Agric. Ecosyst. Environ.* **2012**, *155*, 70–77. [CrossRef]
10. Sánchez-Cañete, E.P.; Barron-Gafford, G.A.; Chorover, J. A considerable fraction of soil-respired CO_2 is not emitted directly to the atmosphere. *Sci. Rep.* **2018**, *8*, 13518. [CrossRef] [PubMed]
11. Boyce, C.K.; Ibarra, D.E.; D'Antonio, M.P. What we talk about when we talk about the long-term carbon cycle. *New Phytol.* 2022; *advance online publication*. [CrossRef]
12. Liu, Z.; Sun, Y.; Zhang, Y.; Qin, S.; Sun, Y.; Mao, H.; Miao, L. Desert soil sequesters atmospheric CO_2 by microbial mineral formation. *Geoderma* **2020**, *361*, 114104. [CrossRef]
13. Banks, E.D.; Taylor, N.M.; Gulley, J.; Lubbers, B.R.; Giarrizzo, J.G.; Bullen, H.A.; Hoehler, T.M.; Barton, H.A. Bacterial calcium carbonate precipitation in cave environments: A function of calcium homeostasis. *Geomicrobiol. J.* **2010**, *27*, 444–454. [CrossRef]
14. Glunk, C.; Dupraz, C.; Braissant, O.; Gallagher, K.L.; Verrecchia, E.P.; Visscher, P.T. Microbially mediated carbonate precipitation in a hypersaline lake, Big Pond (Eleuthera, Bahamas). *Sedimentology* **2011**, *58*, 720–736. [CrossRef]
15. Shi, S.; Tian, L.; Nasir, F.; Bahadur, A.; Batool, A.; Luo, S.; Yang, F.; Wang, Z.; Tian, C. Response of microbial communities and enzyme activities to amendments in saline-alkaline soils. *Appl. Soil Ecol.* **2019**, *135*, 16–24. [CrossRef]
16. Yang, C.; Lv, D.; Jiang, S.; Lin, H.; Sun, J.; Li, K.; Sun, J. Soil salinity regulation of soil microbial carbon metabolic function in the Yellow River Delta, China. *Sci. Total Environ.* **2021**, *790*, 148258. [CrossRef]
17. Liu, Z.; Zhang, Y.; Fa, K.; Zhao, H.; Qin, S.; Yan, R.; Wu, B. Desert soil bacteria deposit atmospheric carbon dioxide in carbonate precipitates. *Catena* **2018**, *170*, 64–72. [CrossRef]
18. Fang, H.; Liu, G.; Kearney, M. Georelational analysis of soil type, soil salt content, landform, and land use in the Yellow River Delta, China. *Environ. Manag.* **2005**, *35*, 72–83. [CrossRef]

19. Bai, J.; Yu, Z.; Yu, L.; Wang, D.; Guan, Y.; Liu, X.; Gu, C.; Cui, B. In-situ organic phosphorus mineralization in sediments in coastal wetlands with different flooding periods in the Yellow River Delta, China. *Sci. Total Environ.* **2019**, *682*, 417–425. [CrossRef] [PubMed]
20. Food and Agriculture Organization (FAO); UNESCO. *Soil Map of the World*; FAO: Rome, Italy, 1978; Volume 1–10.
21. Zhao, Q.Q.; Bai, J.H.; Zhang, G.L.; Jia, J.; Wang, W.; Wang, X. Effects of water and salinity regulation measures on soil carbon sequestration in coastal wetlands of the Yellow River Delta. *Geoderma* **2018**, *319*, 219–229. [CrossRef]
22. Kumar, S.; Stecher, G.; Tamura, K. MEGA7: Molecular evolutionary genetics analysis version 7.0 for bigger datasets. *Mol. Biol. Evol.* **2016**, *33*, 1870–1874. [CrossRef]
23. R Core Team. *A Language and Environment for Statistical Computing*; R Ver. 4.0. 3.; R Foundation for Statistical Computing: Vienna, Austria, 2020; Available online: http://www.R-project.org (accessed on 10 October 2022).
24. Cao, C.; Jiang, J.; Sun, H.; Huang, Y.; Tao, F.; Lian, B. Carbonate mineral formation under the influence of limestone-colonizing actinobacteria: Morphology and polymorphism. *Front. Microbiol.* **2016**, *7*, 366. [CrossRef] [PubMed]
25. Smythe, W.F.; McAllister, S.M.; Hager, K.W.; Hager, K.R.; Tebo, B.M.; Moyer, C.L. Silica biomineralization of Calothrix-dominated biofacies from Queen's Laundry hot-spring, Yellowstone National Park, USA. *Front. Environ. Sci.* **2016**, *4*, 40. [CrossRef]
26. Andrei, A.Ş.; Păuşan, M.R.; Tămaş, T.; Har, N.; Barbu-Tudoran, L.; Leopold, N.; Banciu, H.L. Diversity and biomineralization potential of the epilithic bacterial communities inhabiting the oldest public stone monument of Cluj-Napoca (Transylvania, Romania). *Front. Microbiol.* **2017**, *8*, 372. [CrossRef] [PubMed]
27. Song, H.; Kumar, A.; Zhang, Y. Microbial-induced carbonate precipitation prevents Cd^{2+} migration through the soil profile. *Sci. Total Environ.* **2022**, *844*, 157167. [CrossRef]
28. Ronholm, J.; Schumann, D.; Sapers, H.M.; Izawa, M.; Applin, D.; Berg, B.; Mann, P.; Vali, H.; Flemming, R.L.; Cloutis, E.A.; et al. A mineralogical characterization of biogenic calcium carbonates precipitated by heterotrophic bacteria isolated from cryophilic polar regions. *Geobiology* **2014**, *12*, 542–556. [CrossRef]
29. Balci, N.; Menekşe, M.; Karagüler, N.G.; Şeref Sönmez, M.; Meister, P. Reproducing authigenic carbonate precipitation in the hypersaline Lake Acıgöl (Turkey) with microbial cultures. *Geomicrobiol. J.* **2016**, *33*, 758–773. [CrossRef]
30. Meier, A.; Kastner, A.; Harries, D.; Wierzbicka-Wieczorek, M.; Majzlan, J.; Büchel, G.; Kothe, E. Calcium carbonates: Induced biomineralization with controlled macromorphology. *Biogeosciences* **2017**, *14*, 4867–4878. [CrossRef]
31. Montaño-Salazar, S.M.; Lizarazo-Marriaga, J.; Brandão, P.F.B. Isolation and potential biocementation of calcite precipitation inducing bacteria from Colombian buildings. *Curr. Microbiol.* **2018**, *75*, 256–265. [CrossRef]
32. Okyay, T.O.; Nguyen, H.N.; Castro, S.L.; Rodrigues, D.F. CO_2 sequestration by ureolytic microbial consortia through microbially-induced calcite precipitation. *Sci. Total Environ.* **2016**, *572*, 671–680. [CrossRef]
33. Zhu, T.; Dittrich, M. Carbonate precipitation through microbial activities in natural environment, and their potential in biotechnology: A review. *Front. Bioeng. Biotechnol.* **2016**, *4*, 4. [CrossRef]
34. Bindschedler, S.; Cailleau, G.; Verrecchia, E. Role of fungi in the biomineralization of calcite. *Minerals* **2016**, *6*, 41. [CrossRef]
35. Uren, N.C. Calcium oxalate in soils, its origins and fate—A review. *Soil Res.* **2018**, *56*, 443–450. [CrossRef]
36. Hervé, V.; Simon, A.; Randevoson, F.; Cailleau, G.; Rajoelison, G.; Razakamanarivo, H.; Bindschedler, S.; Verrecchia, E.; Junier, P. Functional Diversity of the Litter-Associated Fungi from an Oxalate-Carbonate Pathway Ecosystem in Madagascar. *Microorganisms* **2021**, *9*, 985. [CrossRef] [PubMed]
37. Syed, S.; Buddolla, V.; Lian, B. Oxalate Carbonate Pathway-Conversion and Fixation of Soil Carbon-A Potential Scenario for Sustainability. *Front. Plant Sci.* **2020**, *11*, 591297. [CrossRef]
38. Paiva, E.A.S. Are calcium oxalate crystals a dynamic calcium store in plants? *New Phytol.* **2019**, *223*, 1707–1711. [CrossRef]
39. Tian, K.; Wu, Y.; Zhang, H.; Li, D.; Nie, K.; Zhang, S. Increasing wind erosion resistance of aeolian sandy soil by microbially induced calcium carbonate precipitation. *Land Degrad. Dev.* **2018**, *29*, 4271–4281. [CrossRef]